Chromosome Extraction and Revision of Linkage Group 2 in *Tribolium castaneum*

R. W. Beeman, J. J. Stuart, M. S. Haas, and K. S. Friesen

We used a balancer chromosome to recover ethylmethanesulfonate-induced recessive mutations in a targeted region of the genome of the red flour beetle (*Tribolium castaneum*) by the technique of chromosome extraction. The experiments reported herein constitute the first successful application of this powerful technique in the order Coleoptera. Using the balancer chromosome *maxillopedia-Dachs3* ($mxp^{Dch\text{-}3}$), we recovered seven recessive visible variants representing seven distinct loci and several dozen recessive lethal variants representing at least five distinct loci after screening 1,607 EMS-mutagenized chromosomes. A subset of the $mxp^{Dch\text{-}3}$-extracted mutations were positioned on the map of the second linkage group by a series of two-, three-, and four-point crosses. The orientation of the homeotic gene complex (HOM-C) on this linkage group was also determined. With the advent of better and more varied balancer chromosomes and the concomitant improvement of chromosome extraction procedures for genetic analysis of *T. castaneum*, saturation mutagenesis of targeted regions of the genome is now feasible in this species.

Drosophila melanogaster offers the preferred experimental system for analyzing the structure and function of insect genes. This is due in part to the ability to conduct saturation mutagenesis and to manipulate chromosomes *in vivo* using balancer chromosomes. However, in view of the great diversity of insect forms and the great importance of insects to mankind, other insect models are clearly needed. Much effort is being devoted to mapping the genomes of several economically important insect species with molecular markers (Hunt and Page 1995; Severson et al. 1993; Zheng et al. 1993) and to developing new techniques for germ-line transformation (O'Brochta and Handler 1993). For most of these species, however, overall poor genetic tractability and, in particular, the absence of methods for chromosome manipulation severely limit the variety of experimental approaches possible.

The red flour beetle (*Tribolium castaneum*) has a number of advantages that recommend it as a favorable subject for genetic and molecular investigations, including ease of rearing, handling, and making genetic crosses; a reasonably short generation time; the existence of a large collection of visible mutations, chromosome rearrangements, and other genetic variants; relatively well-marked linkage maps; and a small genome size with a long-period interspersion pattern of distribution of repetitive DNA (Beeman et al. 1992; Brown et al. 1990; Juan et al. 1993). To date, one of the best characterized genetic regions of the *T. castaneum* genome is the second linkage group (LG2). This has resulted from our analysis of an important cluster of developmental regulatory genes called the homeotic complex (HOM-C), represented by more than 70 mutations (Beeman 1987; Beeman et al. 1989). Our integrated genetic/molecular/developmental analysis of this region has helped to establish *Tribolium* as an important new model for genetic studies and has led to the discovery of several chromosome rearrangements with breaks in or near the HOM-C (Beeman et al. 1986; Stuart et al. 1993). We have used these rearrangements to test the feasibility of chromosome extraction in beetles. Previously we briefly discussed the use of balancers for chromosome extraction (Beeman et al. 1992). In this report we describe in detail the results of our efforts to identify new recessive genetic markers for LG2 by ethylmethanesulfonate mutagenesis followed by chromosome extraction using the balancer chromosome *maxillopedia-Dachs3* ($mxp^{Dch\text{-}3}$).

Materials and Methods

Strains and Genetic Variants

The standard, wild-type strains GA-1 and Lab-S are described in Haliscak and Bee-

From the U.S. Grain Marketing Research Laboratory, Agricultural Research Service, U.S. Department of Agriculture, 1515 College Ave., Manhattan, KS 66502 (Beeman and Haas); the Department of Entomology, Purdue University, West LaFayette, Indiana (Stuart); and the Division of Biology, Kansas State University, Manhattan (Friesen). This research was supported in part by USDA grant no. 92-37302-7605, by NIH grant no. HD29594, and by Midwest Plant Biotechnology Consortium grant no. 593 0038-22.

Journal of Heredity 1996;87:224–232; 0022-1503/96/$5.00

Table 1. Description of visible mutations referred to in this work

Allele	Locus	Origin*	Description (Viable/Lethal)	Original reference
maxillopedia (mxp)	*maxillopedia (mxp)*	S	Weak homeotic transformation of maxillary and labial palps to legs (V)	Sokoloff (1966, 1977)
alate prothorax (Cx^{apr})	*Cephalothorax (Cx)*	S	Weak homeotic transformation of prothorax to mesothorax (V)	Sokoloff (1966, 1977)
pointed abdominal sternite (A^{pas})	*Abdominal (A)*	S	Weak homeotic transformation of abdominal segment 4 to 3 (V)	Sokoloff (1966, 1977)
pointed abdominal sternite ($A^{pas\text{-}2}$)	*Abdominal (A)*	G, GA-1	Strong homeotic transformation of abdominal segment 4 to 3 (V)	Beeman et al. (1989)
Reindeer (Rd)	*Reindeer (Rd)*	S	Thickened antennae and femurs (V)	Dawson (1984)
Recurved anterior pronotum (Rap)	*Recurved anterior pronotum (Rap)*	S, GA-1	Notched anterior border of pronotum (V)	This work
unbuckled (ub)	*unbuckled (ub)*	S, *ab*/$A^{pas\text{-}2}p$	Slender appendages, and epimera folded back and protruding outward from prothoracic sternellum (V)	This work
Eye reduced (Er)	*Eye reduced (Er)*	G, $Cx^{Ag\text{-}1}$	Missing ommatidia and constriction in ocular portion of head; similar to *Ey* (L)	Stuart and Mocelin (1995)
Dachs-3 ($mxp^{Dch\text{-}3}$)	*mxp*	G, GA-1	Weak homeotic transformation of prothorax to labium: short prothoracic legs and reduced pronotum (L)	This work
Extra sclerites ($A^{Ex\text{-}1}$)	*A*	G, GA-1	Strong homeotic transformation of abdominal segment 2 to 3 (L)	Beeman et al. (1989)
Eyeless (Ey)	*microcephalic (mc)*	G, GA-1	Missing ommatidia and constriction in ocular portion of head; similar to *Er* (L)	This work
Stumpy (mxp^{Stm})	*mxp*	EMS, Lab-S	Strong homeotic transformation of antennae to palps: short antennae (SL)	Beeman et al. (1989)
Antennagalea-1 ($Cx^{Ag\text{-}1}$)	*Cx*	G, GA-1	Homeotic transformation of basal antenna to basal maxillary palp (L)	Stuart et al (1991)
Antennagalea-4 ($Cx^{Ag\text{-}4}$)	*Cx*	G, mxp^{Stm}	Similar to $Cx^{Ag\text{-}1}$ (L); small notches in genae	This work
Antennagalea-5 ($Cx^{Ag\text{-}5}$)	*Cx?*	G, mxp^{Stm}	Similar to $Cx^{Ag\text{-}1}$ (L); large notches in genae	This work
Cephalothorax-5 (Cx^{5})	*Cx*	G, mxp^{Stm}	Weak homeotic transformation of prothorax to mesothorax (L), gular sutures unfused	This work
Antennapalpus (mxp^{Ap})	*mxp*	EMS, Lab-S, or GA-1	Homeotic transformation of distal antenna to distal palp (V)	Beeman et al. (1989)
antena bifurcada (ab)	*antena bifurcada (ab)*	S	Long outgrowths on antennae and trochanters (V)	Vasquez and Nunez del Castillo (1985)
pearl (p)	*pearl (p)*	S	White eyes (V)	Sokoloff (1966, 1977)
Pinched sternellum (Ps)	*Pinched sternellum (Ps)*	G, mxp^{Stm}	Malformed sternellum, coxae, and pronotum; branched palps; extra setae (L)	This work

* S = spontaneous, G = gamma radiation-induced; EMS = ethylmethanesulfonate-induced. Strain following comma indicates parent strain.

man (1983). The *sooty* strain (Sokoloff 1966) is homozygous for a spontaneous recessive mutation on LG4 that confers a dark body color. This strain was used for mutagenesis in order to facilitate separation of the sexes after mating. The *ab* strain originated near Bogota, Colombia (Vasquez and Nunez del Castillo 1985), and is segregating for the spontaneous *antena bifurcada* (*ab*) mutation. This variant is recessive and homozygous viable, but is male sterile. The stock is maintained by periodic selection of homozygous, nonvirgin females. General descriptions of other mutations used or referred to in this work are given in Table 1. *Maxillopedia-Dachs3* ($mxp^{Dch\text{-}3}$) was used as the balancer chromosome. The dominant phenotype of $mxp^{Dch\text{-}3}$ is a dramatic shortening and bowlegged appearance of the prothoracic legs (Figure 1C,D) and a reduction in the size of the pronotum due to an apparent gain-of-function mutation of the *maxillopedia* gene in the HOM-C on LG2. This phenotype is easily scorable in larvae, pupae, and adults. The chromosome is lethal when homozygous, and, as shown below, eliminates recovery of viable recombinants over a distance of approximately 25–30 map units on LG2. In addition, the $mxp^{Dch\text{-}3}$ chromosome is associated with pseudolinkage between LG2 and LG9, suggesting that it is a 2,9 translocation (see below). The dominant mutation *Eyeless* (*Ey*) (Table 1) was used in conjunction with $mxp^{Dch\text{-}3}$ for chromosome extraction, as described below. *Ey* is easily scorable in pupae or adults (Figure 1A,B), but is not expressed in larvae. *Ey* is associated with pseudolinkage between LG2 and LG5, and thus appears to be a 2,5 translocation. The *Eyeless* phenotype appears to be caused by a mutation in the *microcephalic* (*mc*) gene on LG5, while the recessive lethality seems to be associated with the LG2 break (Beeman RW, unpublished observations). See Sokoloff (1962) for a description of the *mc* mutation. *Extra sclerites* ($A^{Ex\text{-}1}$) and *Stumpy* (mxp^{Stm}) are dominant, gain-of-function mutations in the homeotic genes *Abdominal* (*A*) and *maxillopedia* (*mxp*), respectively. Both variants suppress recombination in the region of the HOM-C and are balanced by $mxp^{Dch\text{-}3}$. $A^{Ex\text{-}1}$ is associated with pseudolinkage between LG2 and LG4, and thus appears to be a 2,4 translocation. *Cephalothorax* (Cx^{5}) is an apparent null mutation in the homeotic *Cephalothorax* gene, while *Antennagalea-4* ($Cx^{Ag\text{-}4}$) and *Antennagalea-5* ($Cx^{Ag\text{-}5}$) are apparent gain-of-function mutations in the *Cx* gene. Cx^{5}, $Cx^{Ag\text{-}4}$, and $Cx^{Ag\text{-}5}$ were all induced on mxp^{Stm} chromosomes and are all recombinationally inseparable from mxp^{Stm}. As shown below, the two *Ag* variants are associated with regions of crossover suppression considerably more extensive than that of the parent mxp^{Stm} chromosome. The apparent point mutations *Antennapalpus* (mxp^{Ap}), a dominant, gain-of-function *mxp* allele, and the recessive *A* alleles *pointed abdominal sternites* (A^{pas} *and* $A^{pas\text{-}2}$) and

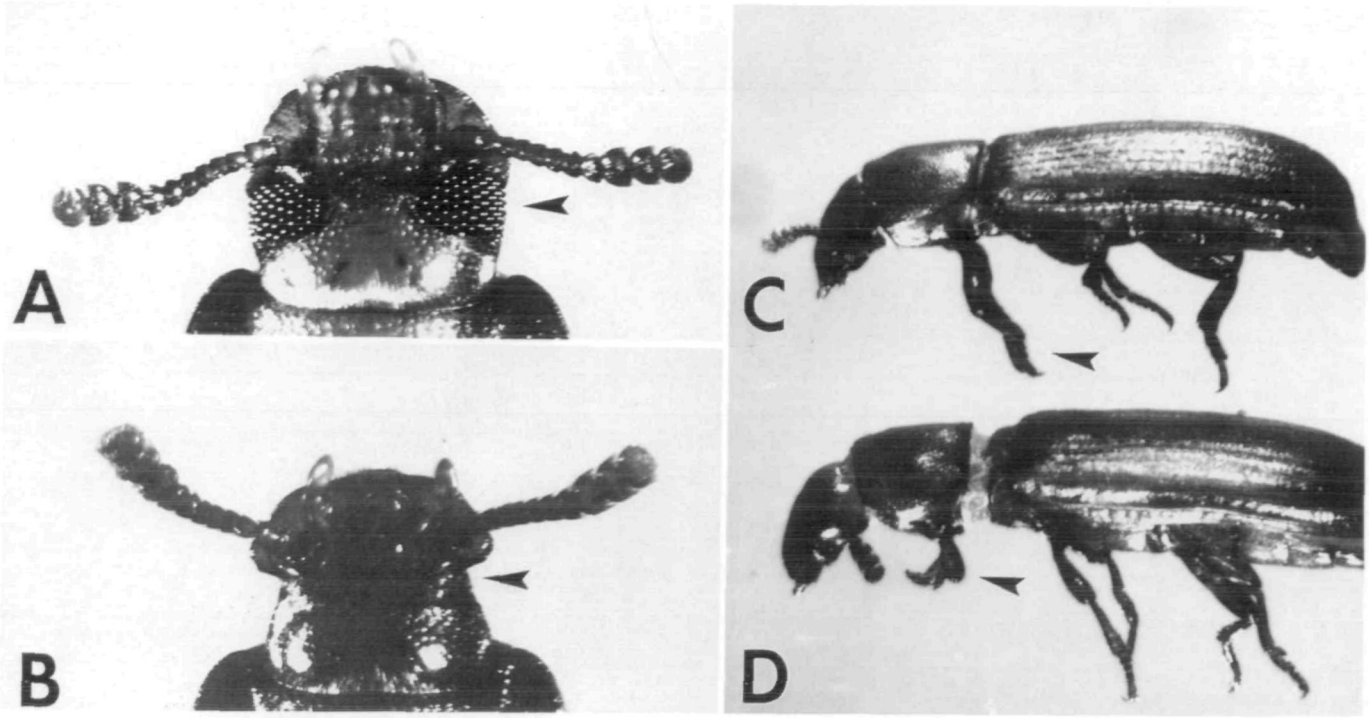

Figure 1. Adult phenotypes of *mxp*$^{Dch\text{-}3}$ and *Ey*. (**A**) Wild-type head, ventral view, showing position of eyes (arrow). (**B**) Corresponding view of *Ey*/+ head, showing constriction resulting from lack of eye development (arrow). (**C**) Side view of wild-type beetle, showing prothoracic legs (arrow). (**D**) Corresponding view of *mxp*$^{Dch\text{-}3}$/+, showing stunted and abnormal development of prothoracic legs (arrow).

missing abdominal sternites (A^{mas}) were used for three- and four-point mapping of extracted mutations.

EMS Mutagenesis

Virgin *sooty* males 2–6 days old were starved overnight, then exposed to 7 cm Whatman #1 filter papers soaked with 2 ml of 1% sucrose + 0.025 or 0.04 M EMS in plastic petri dishes at 100% relative humidity. Males (50 per dish) were allowed to feed on the EMS solution for 24 h in the dark, then were allowed to mate en masse with 2 week old virgin female *mxp*$^{Dch\text{-}3}$/*Ey*. The males were discarded after 3 days. Females were transferred weekly to fresh flour for a total oviposition period of 1–2 months.

1. EMS-fed males X D/E females $\xrightarrow{\text{extract}}$ */D

2. individual */D X D/E $\xrightarrow{\text{amplify}}$ */D

3. */D X self $\xrightarrow{\text{homozygose}}$ */*

Figure 2. General scheme for chromosome extraction of *T. castaneum*. Abbreviations: D = balancer chromosome *mxp*$^{Dch\text{-}3}$; E = dominant marker, *Ey*; * = mutagenized chromosome subject to extraction. In general, D represents any balancer chromosome and E represents any dominant marker included within the balanced region. Cross 1 (extraction) was done en masse. Single */D progeny of this cross, heterozygous for a single, mutagenized second chromosome, were crossed individually to several D/E mates in cross 2 to amplify the extracted chromosome. Several */D sibs (progeny of cross 2), all carrying copies of the same second chromosome, were self-crossed in cross 3 to generate homozygotes. */E progeny of cross 2 were eliminated as larvae to facilitate selection of virgin */D for cross 3. This was made possible by larval expression of the D phenotype.

Chromosome Extraction

We used a standard, three-generation chromosome extraction scheme: (1) extraction of individual mutagenized chromosomes using the balancer chromosome *mxp*$^{Dch\text{-}3}$; (2) amplification of the extracted chromosomes using an additional dominant marker (*Ey*) tightly linked in trans with the balancer chromosome; and (3) rendering the extracted chromosomes homozygous by inbreeding followed by elimination of balancer chromosomes (Figure 2). Specifically, after crossing mutagenized *sooty* males to *mxp*$^{Dch\text{-}3}$ females en masse, virgin F_1 adults heterozygous for *mxp*$^{Dch\text{-}3}$ and for the treated chromosome were individually backcrossed to 2–3 virgin *mxp*$^{Dch\text{-}3}$/*Ey* of the appropriate sex, and virgin progeny heterozygous for *mxp*$^{Dch\text{-}3}$ and for the treated chromosome were mass self-crossed (up to 13 beetles per cross) to generate homozygotes for the treated chromosome. Homozygotes were recognized by the absence of the *mxp*$^{Dch\text{-}3}$ phenotype. Several homozygotes from each line were examined for visible mutant phenotypes. The absence of non-*mxp*$^{Dch\text{-}3}$ phenotypes indicated the presence of a lethal on the mutagenized chromosome. Putative new mutants were confirmed in subsequent generations.

Linkage Group Determination and Mapping of New Mutants

Since *mxp*$^{Dch\text{-}3}$ is a 2,9 translocation (see below), we first had to determine the link-

Table 2. Pseudolinkage of *mxp*$^{Dch\text{-}3}$ with LG9

Progeny phenotype	No. of progeny
D+++	61
+Epa	136
D+p+	5
+E+a	8
D++a	0
+Ep+	0
D+pa	0
+E++	0
DE++	37
++pa	0
DEp+	2
++pa	0
DE+a	0
++p+	0
DEpa	0
++++	0
Total	249

Testcross: D++/+Ep × ap (combined data from 14 single pairs) where D = *mxp*$^{Dch\text{-}3}$, E = $A^{Es\text{-}1}$, p = pearl, and a = $A^{pas\text{-}2}$. $A^{Es\text{-}1}$ and its noncomplementing recessive allele $A^{pas\text{-}2}$ were included to illustrate the nondisjunction invariably associated with *mxp*$^{Dch\text{-}3}$. The DE++ and DEp+ classes reflect this phenomenon. $A^{Es\text{-}1}$ assorts independently of p (Beeman RW, unpublished data).

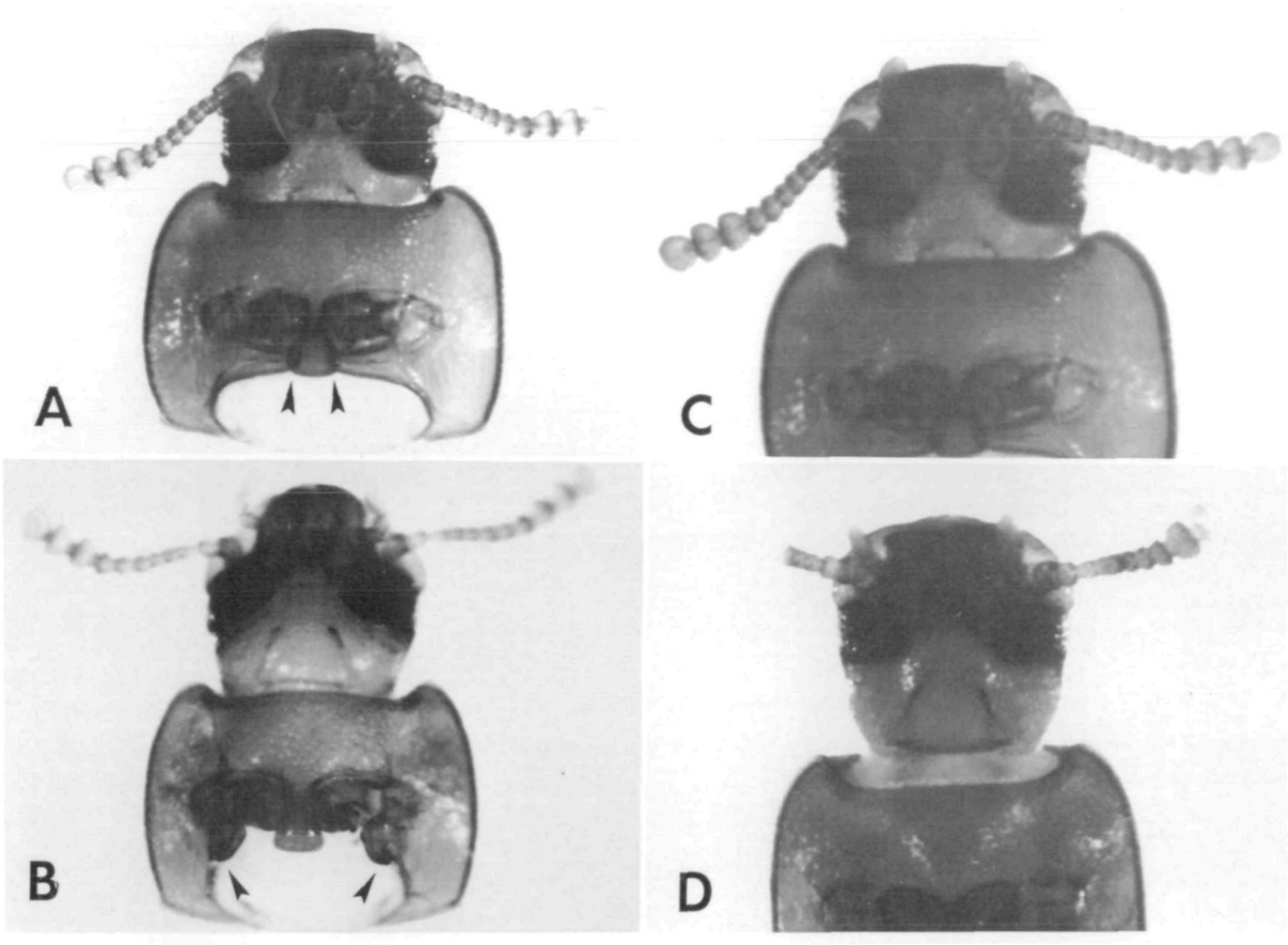

Figure 3. Adult phenotypes of *unbuckled* (*ub*) and *broken antennae* (*ba*). (**A**) Head and prothorax of wild type, ventral view, showing prosternal epimera (arrows) almost joining under the sternellum. (**B**) Corresponding view of head and prothorax of *ub* homozygote, showing prosternal epimera deflected ventroposteriorly. (**C**) Wild type, ventral view, showing 11-segmented antennae. (**D**) *ba* homozygote, ventral view, showing brittle, broken antennae.

Table 3. Orientation of the HOM-C on LG2

Cx-A-ub-Er 4-point cross[a]		*Cx-A-ub* 3-point cross[b]		*Rd-A-Er* 3-point cross[c]	
Progeny phenotype	No. of progeny	Progeny phenotype	No. of progeny	Progeny phenotype	No. of progeny
+++E	284	amu	184	Rm+	67
amu+	218	+++	282	++E	56
a++E	2	a++	4	R+E	26
+mu+	3	+mu	2	+m+	56
am+E	29	am+	16	RmE	2
++u+	14	++u	18	+++	30
amuE	7	a+u	0	R++	1
++++	15	+m+	0	+mE	1
+m+E	0				
a+u+	0				
++uE	0				
am++	0				
a+uE	0				
+m++	0				
+muE	0				
a+++	0				
Total	572	Total	506	Total	239

[a] Testcross was +++E/amu+ × amu.

[b] The testcross was amu+/+++t × amu, where a = alate prothorax (*Cx*^{apr}); m = missing abdominal sternites (*A*^{mas}); u = *unbuckled* (*ub*) and t = *tar*. Phenotypically am+ and ++u crossover progeny were testcrossed to assess the presence of t (see Table 8).

[c] The testcross was Rm+/++E × m, where E = *Eye reduced* (*Er*), R = *Reindeer* (*Rd*), m = *A*^{mas}.

age group assignment for each new mutation. This was done by a series of two-point linkage tests, each involving one of the new mutations and a dominant LG2 marker not pseudolinked to LG9. Males heterozygous for the mutation (*m*) and the dominant LG2 marker chromosome (either *Ey*, *A*$^{Es\text{-}1}$, or *mxp*^{Stm} Cx^{5}) in trans were testcrossed to *m*/*mxp*$^{Dch\text{-}3}$ or homozygous *m* females. For testcrosses to *m*/*mxp*$^{Dch\text{-}3}$ females, only those progeny that inherited the maternal copy of the new recessive variant were scored for recombination. Progeny that inherited the maternal *mxp*$^{Dch\text{-}3}$ chromosome were noninformative and were not included in the analysis. In addition to linkage group assignment, these crosses also established the distance between each new LG2 variant and the HOM-C. Positioning new LG2 variants on the right or left of the HOM-C was accomplished with three-point crosses employing the closely linked homeotic mark-

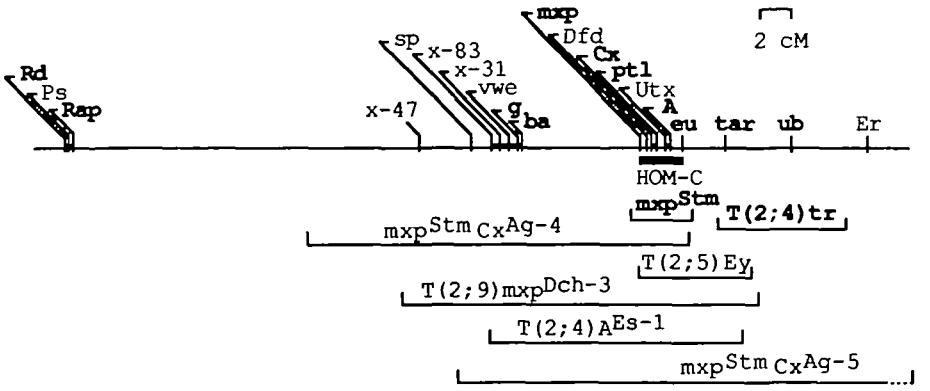

Figure 4. Map of linkage group 2 in *T castaneum*. Scale bar indicates 2 centimorgans (= 2% recombination). Loci represented by at least one adult viable mutation are indicated in bold. An uppercase first letter indicates a dominant allele. The exception is the HOM-C locus *Dfd*, which is known only by molecular mapping based on cross-hybridization with its *Drosophila* homolog (Stuart et al. 1991). The three loci at the far left end of LG2 (*Rd*, *Ps*, and *Rap*) are tightly linked. Double horizontal bars connecting two or more loci indicate uncertainty regarding the gene order. Horizontal brackets below the map indicate regions of crossover suppression associated with the given mutation. Dotted line indicates uncertainty regarding endpoint of crossover suppression.

ers mxp^{Apl} and $A^{pas\text{-}2}$. Mass testcrosses were of the type mxp^{Apl} $A^{pas\text{-}2/m}$ males × $A^{pas\text{-}2}$ females (5–15 males × ca. 50 females). Individual recombinant testcross progeny, derived from meiotic recombination between the mxp^{Apl} and A^{pas30} markers, were scored for the presence of *m* by testcrosses to $m/mxp^{Dch\text{-}3}$.

Results

The Balancer Chromosome $mxp^{Dch\text{-}3}$ is a 2,9 Translocation

Table 2 shows the results of a four-point linkage testcross involving the LG2 variants $mxp^{Dch\text{-}3}$, $A^{Es\text{-}1}$, and $A^{pas\text{-}2}$ and the LG9 variant *p*. Since the three LG2 variants are tightly linked because of the crossover suppression of $mxp^{Dch\text{-}3}$ and $A^{Es\text{-}1}$, the cross is in effect a two-point testcross for pseudolinkage between *p* and the HOM-C region of LG2. It is apparent from these data that $mxp^{Dch\text{-}3}$ and *p* are linked at 6% recombination (15/249). Since *p* assorts independently of $A^{Es\text{-}1}$, $A^{pas\text{-}2}$, and other LG2 variants (Beeman RW, unpublished observations), we conclude that $mxp^{Dch\text{-}3}$ is a 2,9 translocation. At least two other existing rearrangements, $mxp^{Dch\text{-}1}$ and *R(2)2*, are associated with pseudolinkage between the HOM-C region of LG2 and the LG9 marker, *p* (Beeman et al. 1986; Beeman RW, unpublished observations). The existence of DE++ and DEp+ phenotypic progeny classes in Table 2 seems to indicate recombination between D(= $mxp^{Dch\text{-}3}$) and E(= $A^{Es\text{-}1}$). However, a consensus of evidence suggests that these progeny arise not from meiotic recombination, but instead from nondisjunction between the *D* chromosome and its homolog during meiosis. This evidence includes the following: (1) The reciprocal phenotypic classes are not found, and $mxp^{Dch\text{-}3}/A^{Es\text{-}1}$ balanced stocks breed true. (2) The frequency of the presumed nondisjunction class (39/249 = 16%, in Table 2) is much higher than that expected from normal meiotic crossing over within the HOM-C. (3) The DE phenotypic classes lack the a(= $A^{pas\text{-}2}$) phenotype. Normally this phenotype coexpresses with E in E/a beetles because of noncomplementation between the two *A* alleles. The rescue of the *A* phenotype is presumed to occur because of trisomy for the LG2 chromosome as a result of nondisjunction. (4) Presumed nondisjunction progeny are always found in crosses involving the $mxp^{Dch\text{-}3}$ chromosome, and are invariably stunted, malformed, short-lived, and sterile, apparently as a result of aneuploidy.

Table 4. Properties of new, EMS-induced recessive visible mutations identified by chromosome extraction of LG2

New mutation (abbreviation)	Adult viable?	Fertile?	Penetrance (%)	Phenotype
shoulder pads (*sp*)	N	N	100	Gross malformations
glossy (*g*)	Y	Y	100	Smooth, yellow cuticle
broken antennae (*ba*)	Y	Y	99	Discolored, brittle antennae
tar (*tar*)	Y	Y	95	Darkened quinone glands
box (A^{box})	Y	Y*	100	Squared abdomen
tremorous (*tr*)	Y	Y	5–10	Halting, tremorous gait
vestigial wings and elytra (*vwe*)	N	N	100	Vestigial wings and elytra

* Box females are fertile and males are sterile.

Description of the New LG2 Variants *unbuckled* (*ub*) and *Eye reduced* (*Er*)

During the course of this work we found two new LG2 mutations that proved useful in clarifying linkage relationships and defining extents of crossover suppression. *Unbuckled* (*ub*) (Table 1) is a spontaneous recessive mutation found as a small cluster of homozygous adults in the F_2 and F_3 of the cross *ab* × $A^{pas\text{-}2}p$. The mutation was probably preexisting in the *ab* parent strain, a putative mutator stock (Beeman RW, unpublished observations). In *ub* homozygotes, the prosternal epimera are deflected ventroposteriorly away from the body, giving the appearance of having been "pried apart" from their normal position in apposition under the sternellum (Figure 3A,B). Also, the lateral mesothoracic epimera are displaced from the plane of the surrounding sclerites, a condition also associated with certain alleles of the HOM-C gene, *Ultrathorax* (*Utx*). The antennae, legs, and mouthparts of *ub* homozygotes are narrower than those in wild-type beetles, producing a "slender" phenotype. Finally, female *ub* pupae have a small spot of sclerotization or melanization at the midventral anterior margin of the abdominal segment bearing the genital papillae.

The dominant mutation *Eye reduced* (*Er*) (Table 1) was radiation induced on a $Cx^{4s\text{-}01}$ chromosome and was subsequently isolated by recombination. Adults heterozygous for *Er* lack most of the dorsal component of both eyes and the head is reduced behind (posterior to) the gena. Ventral eye development, while also incomplete, is less severely affected, and in contrast to the more extreme phenotype of *Eyeless* (*Ey*), *Er* is most often associated with good bilateral expression of the ventral eye.

Orientation of the HOM-C on LG2

Table 3 shows the results of three- and four-point crosses that reveal the orientation of the HOM-C in relation to *Rd*, *ub*, and *Er*. *Ub* and *Er* are located to the "right" of the HOM-C (Figure 4), approximately 7 and 13 map units, respectively, from A^{mas}. *Rd* is located to the "left" of the HOM-C, approximately 35 map units from A^{mas}. In this context, the HOM-C is drawn with *mxp* on the left and *eu* on the right. The positions of centromeres in relation to linkage maps are unknown for any *Tribolium* link-

age group. An unambiguous linkage group chromosome correlation has been demonstrated only for LG3, which corresponds to the longest autosome, a metacentric (Beeman and Stuart 1990; Mocelin and Stuart 1996). Stuart and Mocelin (1995) have developed a karyotype of *T. castaneum* and have tentatively correlated three additional linkage groups with specific chromosomes.

Description of New Recessive Variants Revealed by Chromosome Extraction

We screened 1,607 EMS-mutagenized chromosomes for visible or lethal mutations after extraction with $mxp^{Dch\text{-}3}$. A total of seven loci represented by recessive visible alleles and five loci represented by recessive lethal alleles were identified. Only one allele within each multiple allelic series was included in the analysis. The visible variants include one new allele at the previously described homeotic *Abdominal* locus and six other mutations representing six new genes (Table 4). Names, abbreviations, and brief descriptions of these seven variants follow: (1) *broken antennae* (*ba*). The distal (club) segments of the antennae of newly eclosed homozygous adults appear pale and unsclerotized. As the beetles age, the club segments remain pale, while the more proximal (funicular) segments become excessively darkened, melanotic, and brittle, eventually breaking off (Figure 3C,D). (2) *tar* (*tar*). The contents of the anterior (prothoracic) quinone gland reservoirs of *tar* homozygotes are more darkly pigmented than those of wild type, usually a red-brown to purple-brown compared to the normal clear to wax-yellow color (Figure 5A,B). Posterior (abdominal) quinone glands are not affected. For the most part, *tar* beetles seem unable to secrete the contents of the affected glands, although secretion from the posterior glands is normal. Even in wild-type beetles the normally clear or yellowish secretion of quinone glands darkens several days after being secreted. Thus, the darker color of *tar* glands may result from oxidation or breakdown of gland contents retained in the body longer than normal because of a defect in the secretion mechanism. In this context, it should be noted that the pitch-black quinone gland contents of beetles homozygous for the unlinked *melanotic stink gland* (*msg*) mutation are secreted at relatively normal levels compared to those of *tar* beetles. (3) *box* (A^{box}). This appears to be a regulatory mutation in the homeotic *Abdominal* (*A*) gene. The posterior abdomens of

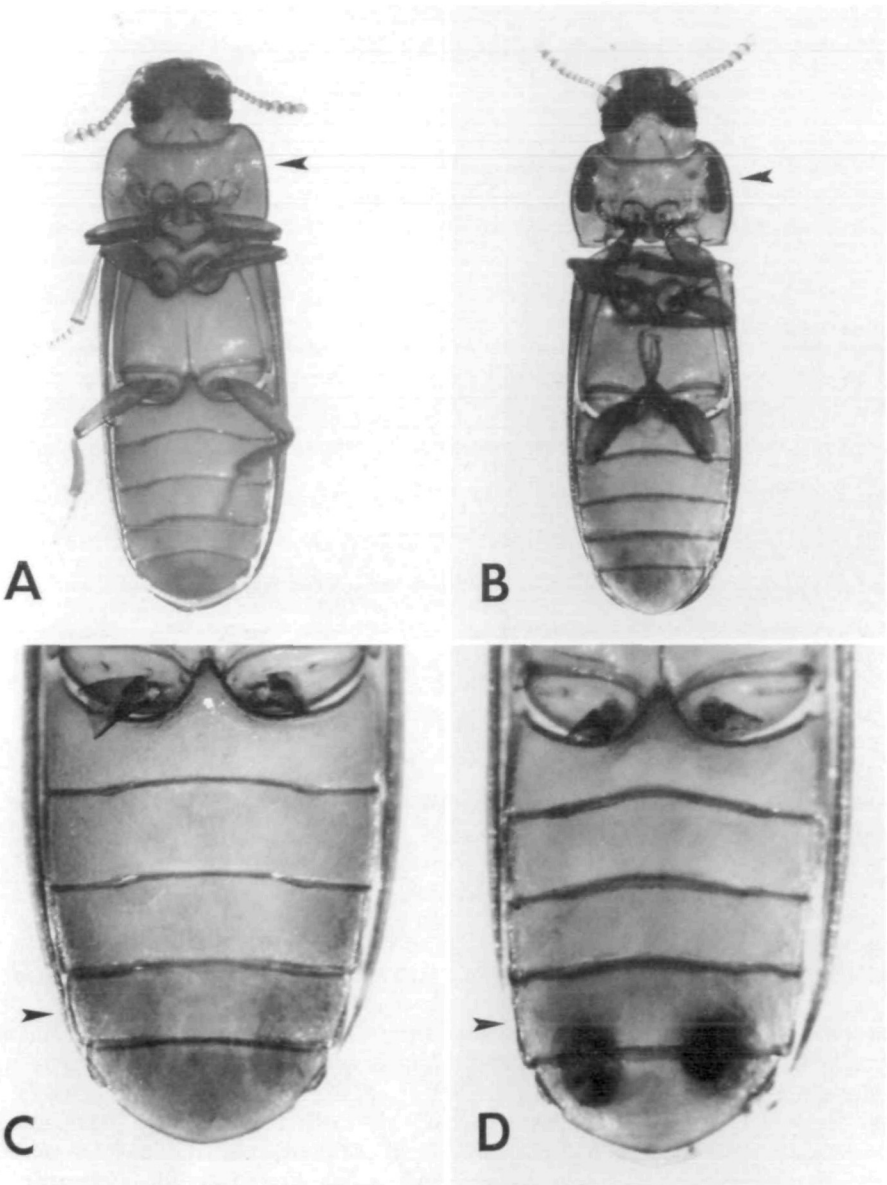

Figure 5. Adult phenotypes of *tar* (*tar*) and *box* (A^{box}). (**A**) Wild-type adult, ventral view, showing position of paired anterior quinone glands (arrow). (**B**) *tar* homozygote, showing melanized quinone gland contents (arrow). (**C**) Wild-type abdomen, ventral view, with the sixth abdominal segment (A6) indicated (arrow). (**D**) Abdomen of A^{box} homozygote, with the enlarged, squared A6 segment indicated (arrow). Note also the melanized contents of the posterior pair of quinone glands.

box homozygous adults are less smoothly tapered than those of wild type. This is due to an anteriorward homeotic transformation of the ventral A5 and A6 sclerites, which are wider and more rectangular than normal, appearing to mimic A4 (Figure 5C,D). *Box* homozygotes also have a *tar*-like phenotype (restricted to the abdominal quinone glands) and appear unable to secrete the abdominal gland contents (see above). Male *box* homozygotes are sterile, while females are fertile. Males have greatly enlarged vasa deferentia, approximately three times greater in diameter than those seen in the wild-type strain Lab-S. Other reproductive structures appear normal. A^{s}/A^{box} heteroallelics have everted quinone glands protruding from between the A6 and A7 sternite (a typical loss-of-function *A* phenotype), and also show a transformation of A5 toward A7 manifested by paired notches along the posterior margin of A5. A^{box} complements both A^{pas} and A^{mas}, apparently a reflection of the complexity of the *A* locus. (4) *vestigial wings and elytra* (*vwe*). Wings and elytra evert from the pupal imaginal discs and begin to differentiate, but their development is arrested at an early stage (Figure 6A). Most adults are inviable, but es-

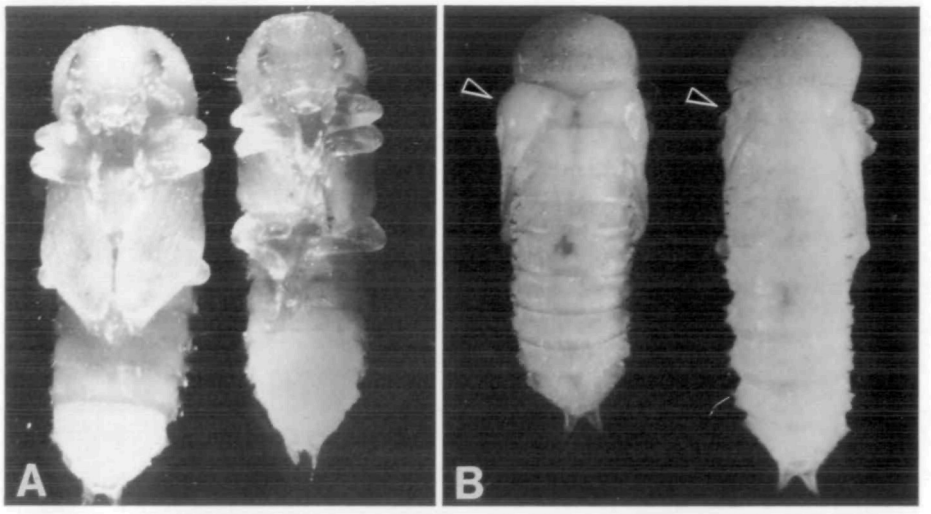

Figure 6. Pupal phenotypes of *vestigial wings* and *elytra* (*vwe*) and *shoulder pads* (*sp*). (**A**) Ventral views of wild-type pupa (left), showing wings and elytra covering the metathoracic legs, and *vwe* homozygote (right), with metathoracic legs exposed. Note the miniature-sized wings and elytra tucked between the mesothoracic and metathoracic legs of the *vwe* pupa. (**B**) Dorsal views of wild-type pupa (right), with base of elytra indicated (arrow), and *sp* homozygote (left), with blisters at the base of the elytra (arrow).

capers are occasionally found with well-differentiated (but miniature-sized) wings and elytra. (5) *shoulder pads* (*sp*). The elytra of *sp* homozygous pupae are malformed proximally, producing an overall appearance of "padded shoulders" (Figure 6B). Homozygous pupae and adults have many other subtle malformations affecting all body regions, and adults are inviable. (6) *glossy* (*g*). The general cuticle, with the exception of the elytra, has a smooth, glossy appearance due to the absence of the normal texture or surface microsculpture between the setiferous pits. In addition, the color of the cuticle is a light pumpkin yellow compared to the slightly darker rust-red color of the wild type. There are also subtle effects on the morphology of certain ventral sclerites. (7) *tremorous* (*tr*). This mutation is associated with a homozygous viable translocation between LG2 and LG4. The break on LG4 is tightly linked in cis to the *sooty* mutation (mutagenized males were already homozygous for this trait). Homozygotes, in addition to the *sooty* phenotype, express a behavioral abnormality that consists of a halting, tremorous gait. This phenotype was strongly expressed in the first several generations of *tr* culture, but more recently has become much less severe and now has ≤10% penetrance.

Two-Point Crosses to Confirm LG2 Linkage of New Recessive Visible and Lethal Mutations

The results of linkage group assignments for six of the seven extracted visible and three of the five extracted lethal mutations are shown in Tables 5 and 6, respectively. Each of the nine mutations tested proved to be linked in trans to one or more of the dominant LG2 markers *Rd, Ey, Er,* $A^{Es\text{-}1}$, mxp^{Apl}, or mxp^{Stm}. In addition, each of the homozygous viable mutations *g* and *ba* were tested for linkage in cis with HOM-C point mutations in separate two-point crosses. The *g*-$A^{pas\text{-}2}$ and *ba-mxp* recombination distances were each found to be 8% (data not shown). The visible mutation

Table 5. Linkage group assignment of recessive visible variants derived by chromosome extraction

Progeny phenotype	No. of progeny for given variant					
	sp	*g*	*ba*	*tar*	*tr*	*vwe*
+D	40	18	25	135	130	104
m+	17	6	36	58	85	25
++	2	1	0	5	1	7
mD	1	0	0	1	1	1
Total	60	25	61	199	217	137
Cm	5	4	0	3	1	6
D =	Ey	Ey	Es	Apl	Apl	Stm

Because of variable penetrance of the *tr* phenotype, the tightly linked cis marker *sooty* was scored instead. Es = $A^{Es\text{-}1}$, Apl = mxp^{Apl}, Stm = mxp^{Stm}.

Table 6. Linkage group assignment of extracted lethals

Lethal	Percent recombination with indicated dominant marker (total no. scored in parentheses)		
	Rd	*Ey*	*Er*
x-31	39 (51)	10 (42)	32 (163)
x-47	19 (152)	19 (53)	30 (86)
x-83	29 (101)	12 (42)	19 (201)

Testcross was *x/D* × *x/Dch3* females (single harems for *Rd* and *Ey*, small mass crosses of 5–20 adults for *Er*). Only non-*Dch* progeny were scored. D = dominant marker (*Rd, Ey,* or *Er*).

A^{box} was not tested to confirm LG2 linkage, but was shown to be an allele of the homeotic LG2 gene *Abdominal,* by its failure to complement A^{g} (see above). Linkages to LG9 were not tested.

Three-Point Crosses to Orient the HOM-C With Each New Mutation

Table 7 shows the results of linkage tests that reveal the orientation of the HOM-C with respect to five of the six new visible mutations that represent previously unknown loci. Recombinant genotypes indicate that *sp, g, ba,* and *vwe* map to the left of HOM-C, whereas *tar* maps to the right of HOM-C. The position of *tr* on the right of HOM-C was deduced from a three-point cross involving *tr,* $A^{pas\text{-}2}$, and *ub* that showed that *tr* and *ub* are tightly linked to each other but recombine with $A^{pas\text{-}2}$ (see below). The evidence for the extents of crossover suppression for *tr* = *T(2;4)tr* and the other five crossover suppressors shown in Figure 4 are given below.

Several pieces of evidence support the placement of *x-31, x-47,* and *x-83* to the left of HOM-C: All three are tightly balanced by $mxp^{Dch\text{-}3}$ but show ≥10% recombination with *Ey* and ≥19% recombination with *Er* (Table 6). Furthermore, all three are tightly balanced by $mxp^{Stm}Cx^{Ag\text{-}4}$, a balancer for

Table 7. Three-point mapping of recessive visible LG2 variants derived by chromosome extraction

Genotype of recombinant chromosome	No. found for given variant				
	sp	*g*	*ba*	*tar*	*vwe*
D+m	0	0	0	3	0
D++	3	0	2	0	1
+rm	2	2	2	0	2
+r+	0	0	0	2	0

D = standard dominant marker; r = standard recessive marker; m = extracted mutation being mapped. Testcross was D r/m × r/r, then recombinant chromosome/r × m/m (or m/Dch for adult inviable variants).

Only D-r recombinants were tested for m. For m = *sp, g, ba, tar,* and *vwe*: D = mxp^{Apl}, r = $A^{pas\text{-}2}$.

Table 8. Three-point mapping of recessive visible LG2 variants derived by chromosome extraction in the region to the right of HOM-C

Genotype of recombinant chromosome	No. found for given variant	
	tar	*trembler*
at+	3	6
a++	2	0
+tu	3	0
++u	1	6
Total	9	12

For *tar*: a = A^{pas}, t = *tar*, u = *ub*.

For *trembler*: a = $A^{pas\text{-}2}$, t = *trembler*, u = *ub*

Testcross was a u/t × au/au, then recombinant chromosome/t × t/t.

the region left of HOM-C (see below). Confirmation that *x-47* maps to the left of HOM-C was obtained from the testcross, *x-47/mxp*^{Apl} Cx^{apt} A^{pas} males × *mxp*^{Apl} Cx^{apt} $A^{pas\text{-}2}$ females. Intra-Hom-C recombinant progeny (phenotypically either + + A^{pas} or *mxp*^{Apl} Cx^{apt} +) were tested for the presence of *x-47* as follows: a single + + A^{pas} recombinant was crossed to *x-47/mxp*$^{Dch\text{-}3}$, and phenotypically *mxp*$^{Dch\text{-}3}$, non-Cx^{apt} progeny were self-crossed in single pairs. Since *mxp*$^{Dch\text{-}3}$ fails to complement Cx^{apt}, these beetles must have carried the + + A^{pas} recombinant chromosome, barring back-recombination. Of two single pairs tested, both bred true for *mxp*$^{Dch\text{-}3}$, indicating the presence of a balanced lethal and demonstrating that the original ++ A^{pas} recombinant carried *x-47* on the crossover chromosome. Two recombinants of the reciprocal phenotypic class, *mxp*^{Apl} Cx^{apt} +, were individually testcrossed to *x-47*/Cx^{apt} *mxp* $A^{pas\text{-}2}$ nonrecombinant siblings, and the fertility of these crosses was measured. Both crosses produced 100% viable progeny (19 and 38 eggs, respectively), indicating the absence of *x-47* on the recombinant chromosome. These results indicate the gene order *x-47, cx, A,* that is, *x-47* to the left of HOM-C as drawn in Figure 4.

Three-Point Crosses to Map New Mutations on the Right of HOM-C

Table 8 shows the results of mapping tests for *tar* and *tr* on the right of HOM-C. Of nine recombination events between $A^{pas\text{-}2}$ and *ub,* five occurred to the right of *tar* and four to the left of *tar.* Thus, *tar* is located roughly equidistant from $A^{pas\text{-}2}$ and *ub.* Of 12 recombination events between $A^{pas\text{-}2}$ and *ub,* all occurred to the left of *tr.* Thus, *tr* is tightly linked to *ub. Trembler* was found to be associated with reduced crossing over (3%) between $A^{pas\text{-}2}$ and *ub,* and in separate tests was found to recombine with *mxp*^{Apl} at a frequency of 1% and with *Er* at a frequency of 1%.

Table 9. Two-point linkage data delimiting crossover suppressor endpoints

Map region		
Marker 1	Marker 2	% recombinant
Ag-4	*Ps*	18
Ag-4	*x-47*	0
Ag-4	*vwe*	0
Ag-4	*Er*	11
Dch-3	*Rd*	41
Dch-3	*x-47*	0
Dch-3	*sp*	0
Dch-3	*ub*	2
Dch-3	*Er*	2
Es	*x-47*	4
Es	*sp*	3
Es	*x-83*	0
Es	*x-31*	0
Es	*Er*	2
Ag-5	*x-47*	3
Ag-5	*Er*	0
Ey	*vwe*	5
Ey	*ub*	2
Ey	*Er*	2
Stm Cx-5	*x-47*	12
Stm Cx-5	*vwe*	11
Stm Cx-5	*g*	6
Stm	*tar*	4
tr	*A*	3
tr	*ub*	0
tr	*Er*	1

Extent of Crossover Suppression for Five LG2 Balancers and *T(2;4)tr*

Table 9 summarizes all evidence bearing on crossover suppressor endpoints as drawn in Figure 4. The most extensive regions of crossover suppression are associated with *mxp*^{Stm}$Cx^{Ag\text{-}5}$ (at least 30 map units), *mxp*$^{Dch\text{-}3}$ (25 map units), and *mxp*-^{Stm}$Cx^{Ag\text{-}4}$ (22 map units). Taken together, these three balancers span a minimum total of approximately 37 contiguous map units, or about 70% of LG2. The estimate for *mxp*^{Stm}$Cx^{Ag\text{-}5}$ is a minimum, since its region of crossover suppression extends up to the right-most marker on LG2.

Discussion

In this work we have demonstrated for the first time the feasibility of using balancers for chromosome extraction in a beetle species. In the process, we updated and improved the detail of the map of visible and lethal LG2 markers of *T. castaneum,* characterized a number of chromosome rearrangements with respect to pseudolinkage and crossover suppression, and identified a number of new candidate balancer chromosomes. We expect that these developments will contribute to understanding and manipulating the *Tribolium* genome in several ways: First, the improved visible map will enhance and corroborate future maps based on molecular markers. This in turn will improve the resolution of efforts to localize specific genes for purposes of mutagenesis or cloning. Second, the availability of a variety of genetically characterized balancers and chromosome rearrangements will facilitate both linkage group assignment (particularly since recombination occurs in both sexes) and chromosome-linkage group correlation. Third, balancer chromosomes make possible the systematic isolation and analysis of individual chromosomes from wild populations, which can then be examined for the presence of transposable elements, selfish genes, or other naturally occurring factors controlling such properties as fitness, pesticide resistance, host-plant virulence, vector competence, or hybrid incompatibility. Fourth, balancer chromosomes will be indispensable tools in the development of transposon-based gene tagging and germline transformation technology, since they will greatly simplify genetic manipulation of tagged chromosomes after transformant selection. Finally, chromosome extraction will make possible the identification of new genetic functions by simplifying the process of recovering recessive mutations. Our initial trial of the chromosome extraction technique has already led to the discovery of new *Tribolium* genes regulating quinone gland chemistry and morphology, cuticle morphology, neuromuscular function, appendage development, and other vital functions.

References

Beeman RW, 1987. A homeotic gene cluster in the red flour beetle. Nature 327:247–249.

Beeman RW, Johnson TR, and Nanis SM, 1986. Chromosome rearrangements in *Tribolium castaneum* J Hered 77.451–456.

Beeman RW and Stuart JJ, 1990. A gene for lindane + cyclodiene resistance in the red flour beetle (Coleoptera: Tenebrionidae). J Econ Entomol 83:1745–1751.

Beeman RW, Stuart JJ, Haas MS, and Denell RE, 1989. Genetic analysis of the homeotic gene complex (HOM-C) in *Tribolium castaneum.* Devel Biol 133:196–209.

Beeman RW, Stuart JJ, Denell RE, McGaughey WH, and Dover BA, 1992. *Tribolium* as a model insect for study of resistance mechanisms. In: Molecular mechanisms of insecticide resistance—diversity among insects (Mullin CA and Scott J, eds). ACS Symposium Series 505; 202–208.

Brown SJ, Henry JK, Black WC III, and Denell RE, 1990. Molecular genetic manipulation of the red flour beetle: genome organization and cloning of a ribosomal protein gene. Insect Biochem 20:185–193.

Dawson PS, 1984. The *Reindeer* mutation and a revision of linkage groups V and X in the flour beetle, *Tribolium castaneum.* Can J Genet Cytol 26:762–764.

Haliscak JP and Beeman RW, 1983. Status of malathion resistance in five genera of beetles infesting farm-stored corn, wheat and oats in the United States. J Econ Entomol 76:717–722.

Hunt GJ and Page RE, 1995. Linkage map of the honey

bee, *Apis mellifera*, based on RAPD markers. Genetics 139:1371–1382.

Juan C, Vazquez P, Rubio JM, Pettipierre E, and Hewitt G, 1993. Presence of highly repetitive DNA sequences in *Tribolium* flour beetles. Heredity 70:1–8.

Mocelin G and Stuart JJ, 1996. Crossover suppressors in *Tribolium castaneum*. J Hered 87:27–34.

O'Brochta DA and Handler AM, 1993. Prospects and possibilities for gene transfer techniques in insects. In: Molecular approaches to fundamental and applied entomology (Whitten M and Oakeshott J, eds). New York: Springer-Verlag; 451–488.

Severson DW, Mori A, Zhang Y, and Christensen BM, 1993. Linkage map for *Aedes aegypti* using restriction fragment length polymorphisms. J Hered 84:241–247.

Sokoloff A, 1962. Linkage studies in *Tribolium castaneum* Herbst. V. The genetics of *Bar eye, microcephalic* and *Microphthalmic*, and their relationships to *black, jet, pearl* and *sooty* Can J Genet Cytol 4:409–425.

Sokoloff A, 1966. The genetics of *Tribolium* and related species. Advanced Genetics, suppl. 1 New York: Academic Press; 25–30.

Sokoloff A, 1977. The biology of *Tribolium*, vol 3. Oxford: Clarendon Press

Stuart JJ, Brown SJ, Beeman RW, and Denell RE, 1991. A deficiency of the homeotic complex of the beetle *Tribolium*. Nature 350:72–74

Stuart JJ, Brown SJ, Beeman RW, and Denell RE, 1993. The *Tribolium* homeotic gene *Abdominal* is homologous to *abdominal-A* of the *Drosophila* bithorax complex. Development 117:233–242.

Stuart JJ and Mocelin G, 1995. Cytogenetics of chromosome rearrangements in *Tribolium castaneum*. Genome 38:673–680.

Vasquez W and Nunez del Castillo F, 1985. Estudios geneticos en *Tribolium castaneum* (Herbst). II. Mutante "*antena bifurcada*" (*ab*). Bol. Dept. de Biolog., Fac. de Cienc., Univ. Nacnl. de Colombia 2(6):9–22.

Zheng L, Collins FH, Kumar V, and Kafatos FC, 1993. A detailed genetic map for the X chromosome of the malaria vector, *Anopheles gambiae* Science 261:605–608.

Received May 17, 1995
Accepted December 31, 1995

Corresponding Editor: Therese Ann Markow